On the Modeling of UAM Aircraft Community Noise in AEDT Helicopter Mode

Stephen A. Rizzi*
NASA Langley Research Center, Hampton, VA 23681, USA

Menachem Rafaelof†
National Institute of Aerospace, Hampton, VA 23666, USA

In contrast to most commercial air traffic today, vehicles serving the urban air mobility (UAM) market are anticipated to operate within communities and be close to the public at large. The approved model for assessing environmental impact of air traffic actions in the United States, the Federal Aviation Administration (FAA) Aviation Environmental Design Tool (AEDT), does not directly support analysis of such operations. Prior work focused on modeling UAM aircraft within AEDT under fixed-wing mode. This paper addresses the modeling of UAM aircraft under helicopter mode, using requisite noise-power-distance data generated through analysis. Results are compared with those from the fixed-wing approach and a hybrid approach. The latter models some flight segments in fixed-wing mode and others in helicopter mode.

I. Introduction

IN the United States, the Federal Aviation Administration (FAA) Aviation Environmental Design Tool (AEDT)[1] is the required tool to assess aircraft noise and other environmental impacts due to federal actions at civilian airports, vertiports, or in U.S. airspace for commercial flight operations. AEDT and prediction tools with the same or similar modeling technologies are used in other countries as well.[2] For fixed-wing aircraft, AEDT calculates various noise metrics using noise-power-distance (NPD) data specific to each aircraft. In its customary mode of operation, the AEDT flight performance model determines the engine power required to execute the specified flight operation. A key assumption is that noise levels are highly correlated with the corrected net thrust of the engines. This allows noise data to be interpolated for power and distance, along with various other adjustments, to estimate the sound exposure at a set of receptors on the ground. For helicopters, AEDT calculates sound exposure using noise-operational mode-distance (still termed NPD) data specific to the vehicle's operational mode, e.g., vertical ascent. The noise data are interpolated for distance only and are used, with adjustments, to estimate the sound exposure at a set of ground receptors. There is no equivalent correlating parameter such as corrected net thrust for the helicopter mode.

There are some obstacles to using AEDT for assessment of community noise due to urban air mobility (UAM) vehicle operations. The first is that while there are NPD data for existing fixed-wing vehicles and helicopters in the databases used in AEDT, there are no available NPD data for UAM vehicles, whether the vehicles are modeled as fixed-wing or helicopter-type vehicles. Secondly, when modeling a UAM vehicle as a fixed-wing type, there are no performance data available to determine required engine thrust, nor is it clear that engine thrust is a good predictor of noise. When modeling a UAM vehicle as a helicopter type, the number of defined operating modes within AEDT is limited to a few that are appropriate for typical helicopter operations but, that may be insufficient for describing UAM operations.

A recent white paper[3] established a set of high-level goals to address key issues associated with UAM noise. One of these goals is to examine UAM fleet noise impacts through prediction and measurement, along with a recommendation that "*Research be conducted to more fully explore limitations in methods for assessing community noise impact of UAM vehicles in their operational environments, and to generate a software development plan that addresses the limitations of current models over time*." Prior work by the authors[4,5] developed the means to assess the noise exposure of point-to-point UAM operations for aircraft modeled as fixed-wing type in AEDT. In those works, the entire point-to-point operation was modeled as a single departure operation that ended at the intended

* Senior Researcher for Aeroacoustics, Aeroacoustics Branch, stephen.a.rizzi@nasa.gov, AIAA Fellow
† Senior Research Engineer, menachemrafaelof@gmail.com

location. This paper describes an approach for modeling point-to-point operations as a helicopter type using a third generation (Gen 3.1.2) NPD database[6] based on source noise predictions using the NASA second-generation Aircraft Noise Prediction Program (ANOPP2).[7] To adhere to the AEDT rules governing helicopter operations, each point-to-point operation was segmented into a set of departure, overflight, and approach operations. The noise exposures so computed are referred to as the Gen 3 assessments. This paper also describes a hybrid approach in which some segments are modeled in fixed-wing mode and others modeled in helicopter mode. The noise exposures so computed are referred to as the Gen 3A assessments.

II. Concept Vehicle, Operating States, and NPD Data Generation

A. Vehicle Description

The quadrotor reference vehicle developed under the NASA Revolutionary Vertical Lift Technology (RVLT) Project was considered in this study, see Figure 1. The vehicle was sized for a 1200 lb. payload (up to six passengers) executing a representative mission profile.[8] It is an all-electric variant, with four three-bladed rotors, gross weight of 6469 lb., and maximum airspeed V_{max} of 109 knots true airspeed (KTAS). Additional details can be found in Silva et al.[9]

B. Operating States

Trajectory data from a set of operational scenarios with multiple vertiports were used in the Gen 1[4] and Gen 2[5] analyses. These data were reduced to determine aircraft operational states for which noise estimates are needed. The aircraft operating states are defined by pairs of airspeed (knots) and climb angle (degrees). These comprise 42 unique operating states and are binned in 10-knot increments of airspeed (from 0 to 85% of V_{max}) and in 5° increments of climb angle (from -90° in vertical descent, to 90° in vertical ascent). Because the source noise prediction process can be computationally intensive, only those operating states having at least 10 occurrences in the Gen 1 trajectory data were evaluated. The set of Gen 1 operating states was compared with operating state data derived from the Gen 2 trajectory data and was found to adequately cover the range of conditions, see Figure 2. Source noise data for operating states with airspeeds less than 5 knots were computed with zero airspeed, irrespective of climb angle.

Figure 1: NASA RVLT quadrotor reference vehicle.

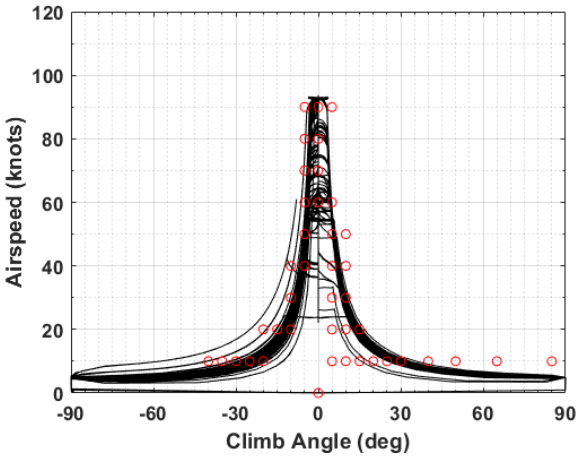

Figure 2: Operating states for the quadrotor vehicle. Black lines represent the Gen 2 trajectory data and red circles represent operating states identified in the Gen 1 study.

For the Gen 3.1.2 NPD database,[6] an additional operating state corresponding to the helicopter "Flight Idle" operational mode was added for both vehicles. Although not occurring in the Gen 1 or Gen 2 trajectory data, either this state or the "Ground Idle" state is required in the database for modeling helicopter departure and approach profiles within AEDT.

C. Noise-Power-Distance Data Generation

The process for generating both fixed-wing and helicopter NPD data was previously documented in detail.[6] The major steps include vehicle trim, source noise definition, and flyover simulation. These processes are reviewed briefly. The first set of operations for generation of source noise data includes vehicle trim and rotor noise analyses and is depicted in Figure 3. The wrapper script "pyaaron" executes all steps for each operating state.

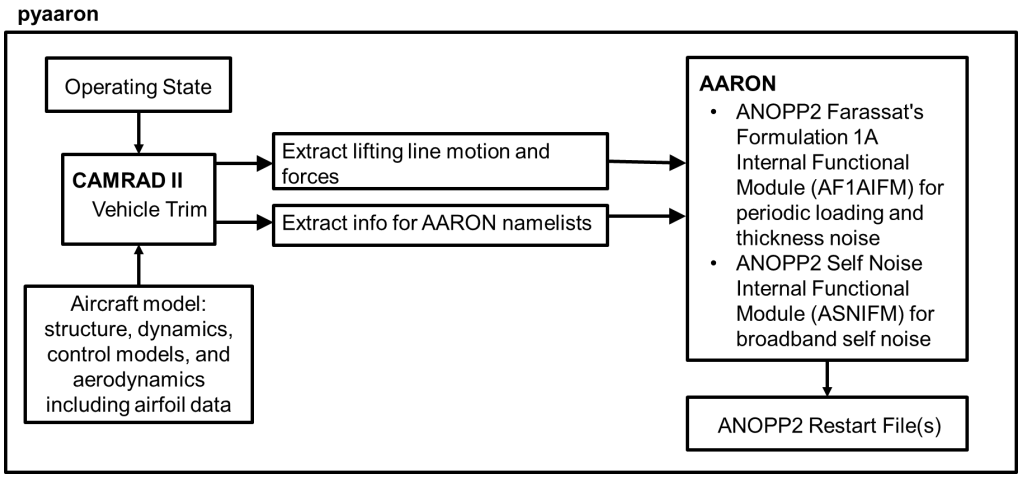

Figure 3: NASA process for generating source noise data for each operating state.

1. Vehicle Trim

The Comprehensive Analytical Model of Rotorcraft Aerodynamics and Dynamics (CAMRAD II)[10] computer program was used to trim the vehicle. In the trimmed condition, the configuration of the vehicle corresponds to the specified operating state (airspeed and climb angle). The rotors on the quadrotor vehicle operate at a constant RPM with a 20 Hz blade passage frequency (BPF) and utilize collective pitch control for all operating states. For each condition, CAMRAD II provides the lifting line geometry and motion to both the compact loading and compact thickness models and the forces acting on the lifting line to the compact loading model. It also provides the angle of attack and the three components of wake-induced fluid velocity as a function of rotor blade radial station and azimuth. These serve as inputs to rotor source noise prediction modules.

2. Rotor Noise Analyses

Rotor source noise data were generated using the ANOPP2 Aeroacoustic ROtor Noise (AARON) tool. Two noise sources were included in the Gen 3.1.2 database. Farassat's Formulation 1A,[11] incorporated in the ANOPP2 Formulation 1A Internal Functional Module (AF1AIFM),[12] was used to compute the periodic loading and thickness noise components under each quasistatic operating condition. The compact thickness and compact loading version of AF1AIFM[13] was used for all source noise calculations. Broadband self noise data were generated using the ANOPP2 Self Noise Internal Functional Module (ASNIFM), following the semiempirical formulations by Brooks et al.[14]

Source noise data were generated in the range of 10 Hz to 5 kHz by AARON for each operating state on a hemisphere of observers centered about the center of gravity of the vehicle at 10° increments in polar angle (fore-aft) and azimuthal angle (port-starboard). A hemisphere radius of 500 ft. (about 38 times the radius of each rotor) was used to ensure that the generated data are in the acoustic far field. The set of observers on the hemisphere move with the vehicle, and therefore, do not include the Doppler frequency shift that would be experienced by a stationary ground observer. The source noise data were written to ANOPP2 restart files for subsequent calculation of NPD data.

3. Simulation of Noise-Power-Distance Data

A list of helicopter operational modes is provided in Table 1. Each set of helicopter NPD data consists of noise metrics as a function of observer distance for each operational mode. For dynamic operational modes, these include maximum metrics (the maximum A-weighted sound pressure level L_{Amx} and the maximum tone-corrected perceived noise level L_{PNTSmx}), and time-integrated exposure metrics (the A-weighted sound exposure level L_{AE} and the effective tone-corrected perceived noise level L_{EPN}). For static operational modes, these include only the maximum metrics, with exposure metrics calculated within AEDT based on the user-specified duration of the operation. Each metric is calculated at the AEDT distances (the "distance" in NPD) of 200, 400, 630, 1k, 2k, 4k, 6.3k, 10k, 16k, and 25k ft. There may be as many helicopter NPD data sets as there are operational modes. Different simulation processes (described below) are used for generation of dynamic and static helicopter NPD data.

AEDT will substitute modes (in some cases with mode-specific dB adjustments) for those that are missing from the NPD database, as indicated in the rightmost column in Table 1. Manufacturer-supplied helicopter NPD data in

AEDT are typically limited to the minimum set of five operational modes, i.e., modes A, D, L, G or H, and I or J, with 0 dB mode-specific adjustments for missing modes. Accordingly, NPD data in this work were generated for only the boldfaced modes in Table 1. Even if all 16 operational modes were supplied, it is immediately apparent that some condensation of source noise data from the 43 operating states identified above is required. Casting of those operating states into a relatively small number of allowable helicopter operational modes is driven, in part, by condensation considerations, which are treated differently depending on the mode.

Table 1: AEDT helicopter operational mode procedural steps.

Operational Mode	Description	State	Substitute Mode
A	**Approach at constant speed**	**Dynamic**	**—**
B	Approach with horizontal deceleration	Dynamic	A + Adj.
C	Approach with descending deceleration	Dynamic	A + Adj.
D	**Departure at constant speed**	**Dynamic**	**—**
E	Depart with horizontal acceleration	Dynamic	D + Adj.
F	Depart with climbing acceleration	Dynamic	D + Adj.
L	**Level flyover at constant speed**	**Dynamic**	**—**
T	Taxi at constant speed	Dynamic	H/I
G	Ground idle	Static	H
H	**Flight idle**	**Static**	**G**
I	Hover in ground effect	Static	J
J	**Hover out of ground effect**	**Static**	**I**
V	Vertical ascent in ground effect	Static	I + Adj.
W	Vertical ascent out of ground effect	Static	J + Adj.
Y	Vertical descent in ground effect	Static	I + Adj.
Z	Vertical descent out of ground effect	Static	J + Adj.

Dynamic Operational Modes

The simulation process used to generate dynamic mode NPD data is incorporated into the ANOPP2 Mission Analysis Tool (AMAT) and is shown in Figure 4. Following the loading of an ANOPP2 restart file (containing the source noise data associated with a single operating state), Doppler frequency shift is applied using the ANOPP2 Wind Tunnel and Flight Effects Internal Functional Module (AWTFEIFM). Three sets of noise metrics are needed as a function of the AEDT reference distances: one set along the centerline and one each at ± 45° azimuth angles to represent lateral directivity. The source noise data are "flown" via simulation at the intended operating state (airspeed and climb angle) using the ANOPP2 Straight Ray Propagation Internal Functional Module (ASRPIFM). By specifying uniform atmospheric conditions, different slant range distances, d, may be computed by a simple change in altitude. International Standard Atmosphere conditions at sea level [1 atm pressure, 59 °F (15 °C) temperature, 0.076 lb/ft^3 (1.225 kg/m^3) air density] and 70% rel. humidity were specified, and a flow resistivity of 250 kRayls, corresponding to grass, was used for the soft ground impedance. A receiver time interval of 0.5 s is used in ASRPIFM to generate a set of one-third octave band SPL spectral data at the ground observer, and noise metrics are calculated using the ANOPP2 Acoustic Analysis Utility (AAAU).

Operating states with zero climb angle and nonzero speed are classified as flyover operational modes L. Mode L NPD data were simulated for all such states. Those operating states with positive climb angle are classified as departure operational modes D and those with negative climb angle are classified as arrival operational modes A. Mode D NPD data were simulated for all operating states with positive climb angles of 5, 10, and 15°. The limitation on climb angles above 15° was made to ensure that the advancing side 10 dB down point needed for noise exposure metrics is met for the shorter AEDT reference distances. This is a conservative estimate made on the assumption of a monopole source and spherical spreading loss only. Within AEDT, the higher climb angles are cast as vertical ascent modes V/W, which are substituted per Table 1 for hover modes I/J. For a similar consideration as mode D, mode A NPD data were simulated for all operating states with descent angles 5, 10, and 15°. Within AEDT, the higher descent angles are cast as vertical descent modes Y/Z, which are substituted per Table 1 for hover modes I/J.

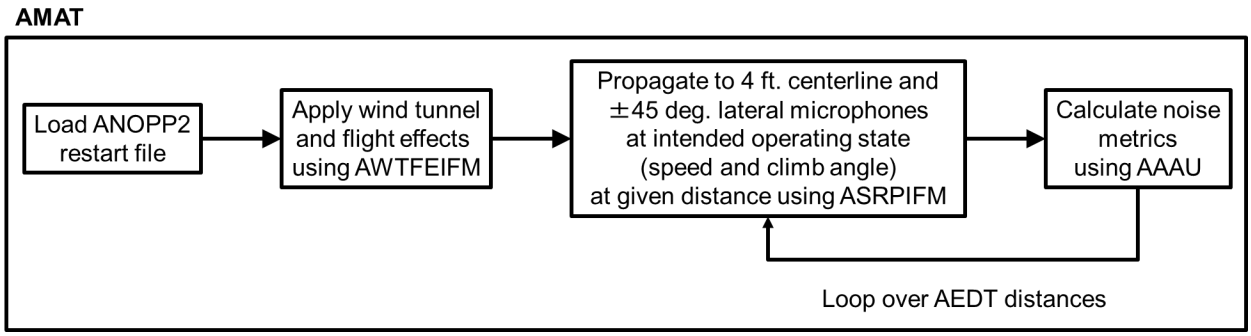

Figure 4: Computational steps in AMAT for generating helicopter NPD data for dynamic operational modes A, D, and L.

With the above limits on climb angle, there are 4, 14, and 10 operating states classified as operational modes L, D, and A, respectively. Within AEDT however, only one operational mode is permitted for each of modes L, D, and A. Therefore, condensation is necessary to reduce the plurality of operational modes to a single mode L, D, and A. The advancing tip Mach number adjustment[1] was used to condense multiple mode L data to a single mode L with second-order polynomial regression coefficients at a reference speed of 90 knots,[6] corresponding to the most prevalent cruise speed. The 90 knot mode L data are shown for the centerline, and port and starboard sides at ± 45° azimuth angles in Figure 5. The data are symmetric about the centerline and the centerline is about 5 dBA higher than the data at ± 45° azimuth angles. Note that the centerline mode L data are the same as the fixed-wing data when the AEDT duration adjustment is applied. On the basis of the NPD data alone, this means that along the centerline (below the track), differences between fixed-wing and helicopter exposure data will be small and increase astride the track up to about 5 dBA (at the 45° azimuth angles), then remain constant further astride, according to the AEDT directivity adjustment for helicopters. The regression coefficients for the advancing tip Mach number adjustment are provided in Table 2.

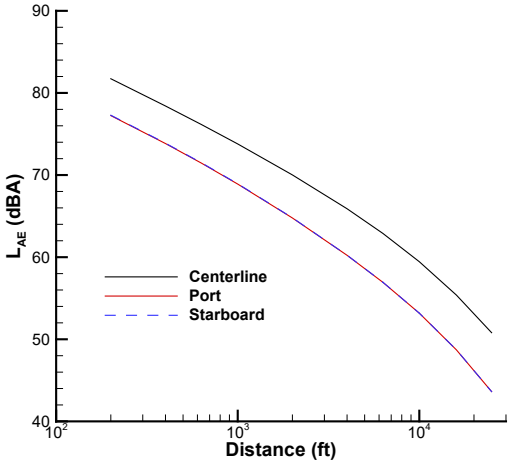

Figure 5: Simulated L_{AE} data for mode L at three microphone locations.

Microphone Location	Coefficients		
	B_0	B_1	B_2
Center	79.63	76.28	0
Left	73.48	10.42	0
Right	73.51	10.28	0

Table 2: Regression coefficients for the advancing tip Mach number adjustment.

There is no condensation method available for modes D and A, so a single mode best representing each set of modes was selected. Simulated L_{AE} data for modes D and A are shown in Figure 6 for the centerline microphone location. The modes D and A centerline data are also higher than the data at the 45° azimuth angles (not shown). The plot legends designate the airspeed (V) in knots and the climb angle (A) in degrees. The mode D data are clustered within a range of about 9 dBA. Being in the middle of the group, the V20 A10 data were selected to represent the single D mode in subsequent analyses. In comparison to the mode D data, the mode A data are at higher levels due to induced blade-vortex interaction noise in descent. While the set of curves is nearly parallel (so-called 'offset' curves), the spread between the low and high noise conditions is about 12 dBA. The V20 A-10 data, being in the middle of the set, were selected to represent the single A mode in subsequent analyses.

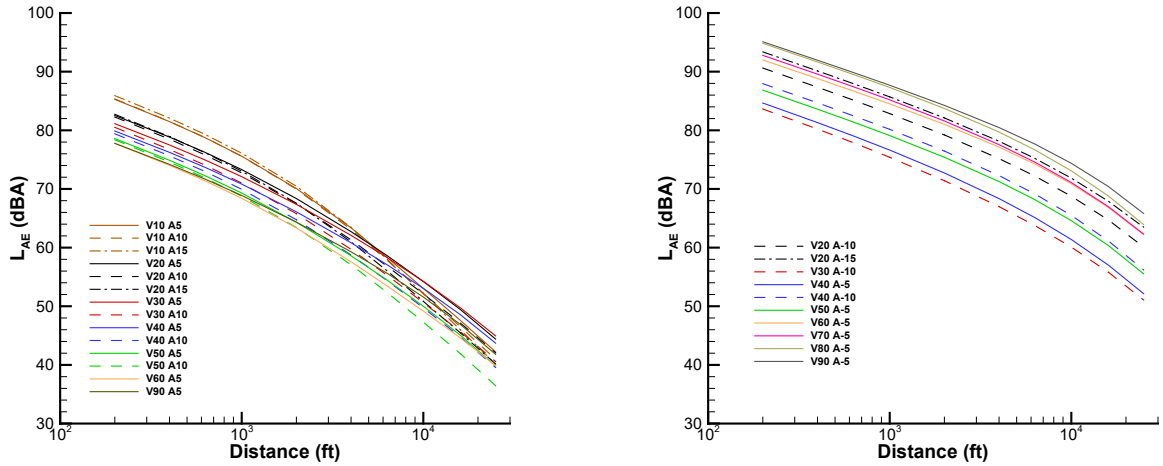

Figure 6: Simulated L_{AE} data for modes D (left) and A (right) at the centerline microphone location.

Static Operational Modes

The computational steps for generating helicopter NPD data for static operational modes differ from those used for dynamic modes, see Figure 7. Since the source and observer are stationary, there is no need to apply Doppler frequency shift prior to propagation. For each mode, a single set of maximum level noise metrics is provided as a function of the AEDT reference distances at locations directly in front of the vehicle. AEDT input for static modes includes the duration of the operation in order to calculate the time-integrated exposure metrics. Mode-specific directivity adjustments are computed relative to the sound level directly ahead of the vehicle for a ring of azimuthal observers (in 15° increments) at a distance of 200 ft.

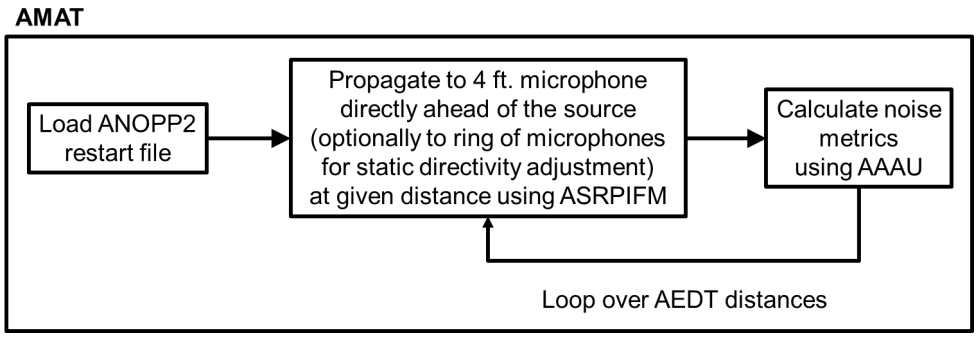

Figure 7: Computational steps in AMAT for generating helicopter NPD data for static operational modes G, H, I, and J.

The method for calculating NPD data for modes G (ground idle) and H (flight idle) is the same; it is only the source noise data that differ. Given that the aircraft of interest are electrically powered, the ground idle operational mode procedural step may not be applicable. However, this mode is required input to AEDT for helicopter departure and approach operations. When absent, the flight idle mode is the default substitution. The corresponding source noise data were obtained with the ground effect model of CAMRAD II enabled.

The method for calculating NPD data for modes I (Hover in Ground Effect) and J (Hover out of Ground Effect) is also the same; it is only the source noise data that differ. Within AEDT, the selection of modes I and J (as well as modes V and W, and modes Y and Z) is dictated by the ground effect altitude (in feet above field elevation), which is equal to 1.5 times the main rotor diameter for helicopters. If the procedural step is below the ground effect altitude, operational mode I (V and Y) is used. Otherwise, operational mode J (W and Z) is used. Since the applicability of the "helicopter ground effect altitude" criterion for UAM vehicles is questionable, only NPD data for mode J were calculated. When mode I is required within AEDT, it is provided by substitution, see Table 1. The main rotor diameter consequently has no effect on discriminating between modes I and J in this case. The operating state of zero airspeed and zero climb angle is used for mode J, see Figure 2. The corresponding source noise data were obtained with the ground effect model of CAMRAD II disabled. Additional details are provided by Rizzi et al.[6]

III. Helicopter Operations Modeling

The starting point for modeling helicopter operations is the previous AEDT study data that modeled UAM flight operations using the fixed-wing aircraft type with fixed-point flight profiles.[4] In that approach, the AEDT study data consist of the airport definition (latitude, longitude, elevation, and runways), fixed-wing NPD data for each vehicle,[6] a set of track points defining the two-dimensional routes along the ground, and a set of profile points defining the aircraft operational state (airspeed and operating state identifier) as a function of altitude above field elevation and the cumulative distance along the track. The profile data include 'guard' points needed to ensure constant operational states along the majority of each segment. The operational state identifier is an index to the fixed-wing NPD data for the specified operational state. In the prior work, each flight was modeled as a single departure operation that simply ends at the intended location. Using the prior fixed-wing data as the starting point helps ensure comparability with the current helicopter analyses.

Aside from establishing helipads in lieu of runways in the airport definition and use of helicopter NPD data instead of fixed-wing NPD data, modeling point-to-point UAM flight operations entails steps for preprocessing the fixed-wing profile data, operational segmentation, casting of profiles into helicopter procedural steps, and study construction. Each set of steps is discussed next.

A. AEDT Procedural Step Rules

Construction of helicopter flight profiles in AEDT requires that a set of rules be followed regarding the prescription of each operational mode procedural step as well as the allowable sequence of procedural steps. The 16 helicopter operational mode procedural steps are listed in Table 1. The rules are detailed in the AEDT user manual[15] and are summarized here.

There are three types of helicopter flight operations that are relevant to this work, namely, departure, overflight, and approach. Each flight operation type must follow a prescribed set of operational mode procedural steps, i.e., there is a particular sequence of steps that must be followed, and not all procedural steps may be specified for every flight operation type. The allowable step transition for departure flight operations is shown in Figure 8. The ellipses are the allowable procedural steps; the arrows indicate valid transitions between steps; an arrow looping back indicates the step can be repeated; the steps within dashed boxes are optional; and one or more steps within the solid boxes are required. The red-boxed letters provide a shorthand version of the procedural step, per Table 1. This figure indicates that a simple departure operation may be constructed from the following sequence of operational mode procedural steps: *ground idle* (G) → *flight idle* (H) → *departure with climbing acceleration* (F) → *level flyover with constant speed* (L). The inclusion of an *approach with descending deceleration* (C) step would not be, for example, allowed at any point in the sequence. The allowable step transition for overflight is shown in Figure 9. This figure removes some of the ambiguity associated with the version provided in the AEDT user manual.[15] Finally, the allowable step transition for approach is shown in Figure 10. An additional *start* (S) procedural step is used to specify the initial altitude and airspeed for overflight and approach operations only.

Each procedural step, except for S, requires specification of one or more of the following parameters: track distance (feet), duration (sec), final altitude (feet) and final airspeed (knots true airspeed, KTAS). The particular parameters vary with procedural step[15] and are not listed here for brevity. Further, AEDT enforces an implicit set of step-specific rules for acceptable values of each parameter. For example, for procedural step C, *approach with descending deceleration*, the final altitude must be lower than the final altitude from the previous step (descending), and the final airspeed must be less than the final airspeed from the previous step (deceleration).

Since the initial track and profile data from the prior fixed-wing analyses were based on finely sampled (1 Hz) simulation data, small variations in airspeed and altitude from one segment to another could potentially violate AEDT rules, i.e., generate AEDT procedural steps or step sequences that are not allowed. To address airspeed exceptions, the average speed along each flight segment in the fixed-wing profile data was discretized into 3-knot bins. This had the desired effect of eliminating most violations. There were no instances of small altitude variations that violated the AEDT parameter rules, so no discretization of altitude was required. There were, however, two mode violations, a decelerating climb and an accelerating descent, that could not be addressed with these simple preprocessing measures. The remedial actions necessary for these violations are described in the next section.

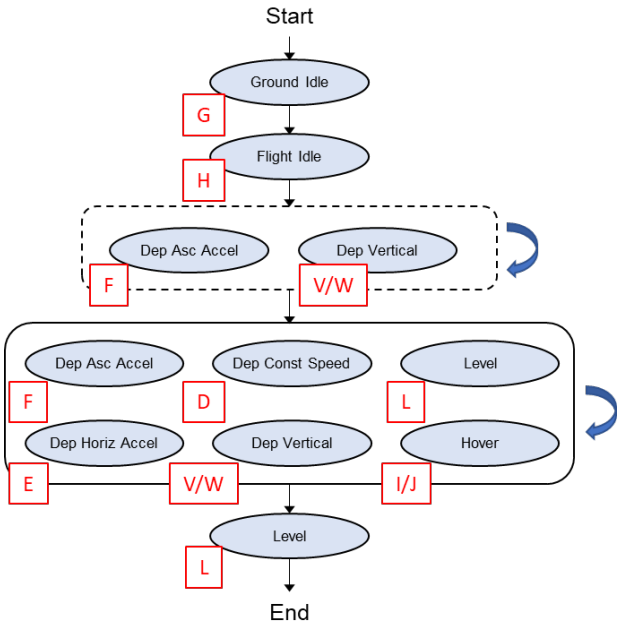

Figure 8: AEDT helicopter departure step transition diagram (adapted from Figure L-7[15]).

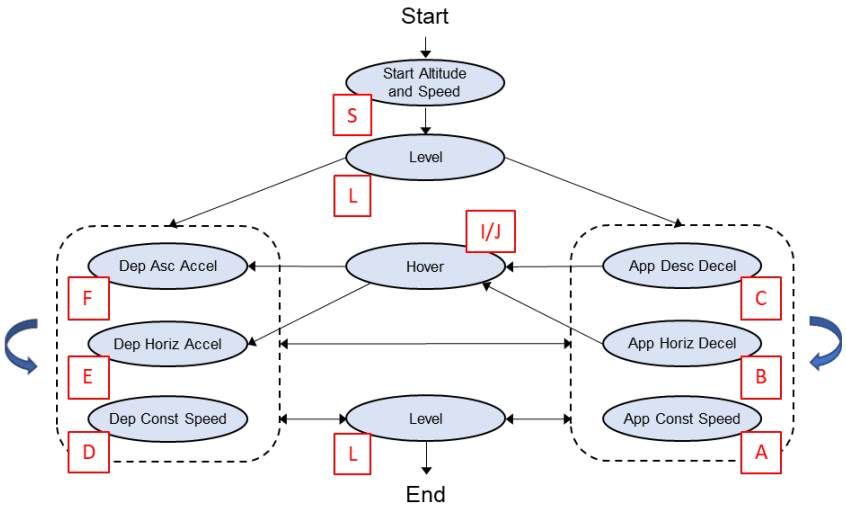

Figure 9: AEDT helicopter overflight step transition diagram (adapted from Figure 3[16]).

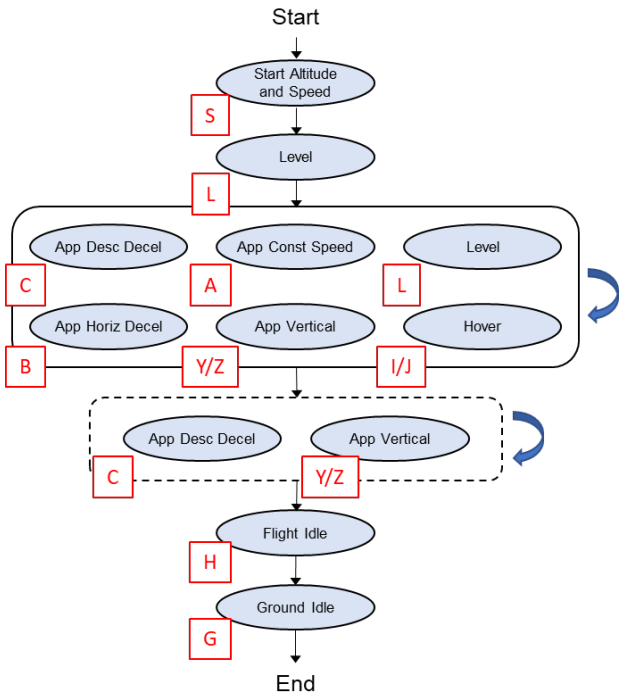

Figure 10: AEDT helicopter approach step transition diagram (adapted from Figure L-6[15]).

B. Operational Segmentation

Because departure, overflight, and approach operations are not individually capable of handling all needed procedural steps for point-to-point operations, each single point-to-point operation was segmented into three separate operations (one for departure, one for overflight, and one for approach) that together are capable of handling all the needed procedural steps. An automated process for operational segmentation is discussed next.

Departure operations are associated with the originating helipad and end with the level flight segment preceding the first instance of an airspeed or altitude decrease, either of which would violate the allowable departure step transitions indicated in Figure 8. The altitude parameter is specified in feet above field elevation (AFE), referenced to the originating helipad. The end of the departure operation marks the start of the overflight operation. The overflight operation ends with the level flight segment following the last case of a speed or altitude increase, the inclusion of which would violate the allowable approach step transitions indicated in Figure 10. Because the overflight operation is referenced to neither the originating nor destination helipad internal to AEDT, the altitude parameter is specified in feet above mean sea level (MSL). The end of the overflight operation marks the start of the approach operation that is associated with, and terminates at, the destination helipad. The altitude parameter is specified in feet above field elevation (AFE), referenced to the destination helipad. Note that this process may result in cases where the identified start of approach (end of overflight operation) precedes the identified end of departure (start of overflight operation). In such cases, the end of departure is simply moved to an arbitrary point preceding the identified start of approach.

It should be apparent that each point-to-point operation will have varying length departure, overflight, and approach operational segments. This is illustrated by the Gen 1^4 data, in which the lengths of the departure, overflight, and approach operations for route KDF4 to KCAT differ from those for route KCAT to KDT4, see Figure 11. The route KCAT to KDT4 is an example of a case in which the initially identified start of approach preceded the initially identified end of departure. The end of departure was subsequently moved to a point preceding the start of approach (as shown).

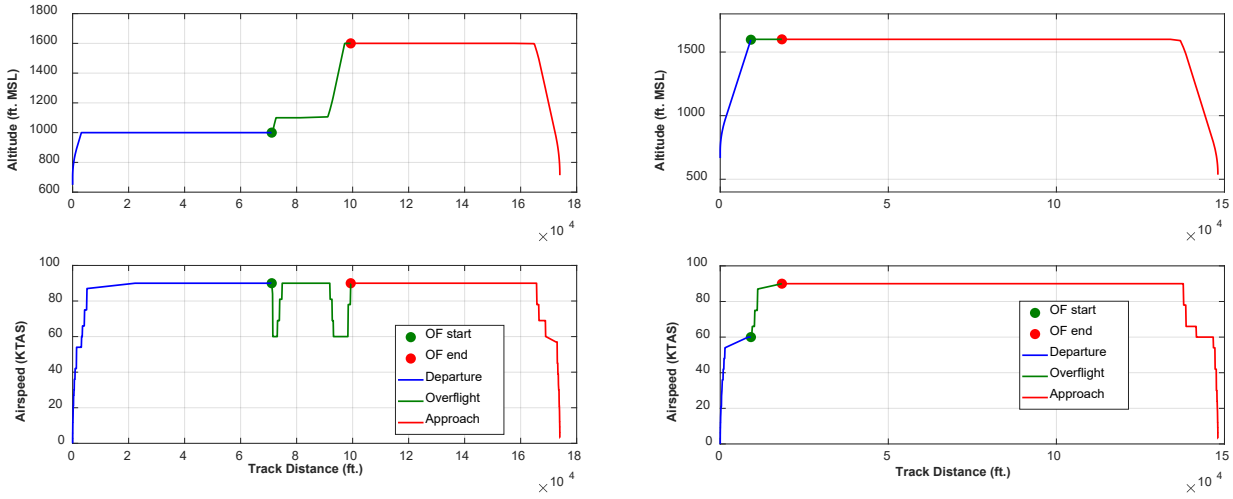

Figure 11: Segmented operations of quadrotor on route KDF4-KCAT (left) and route KCAT-KDT4 (right). The overflight (OF) start and end points differ between routes.

When modeling hybrid operations, in which the fixed-wing mode is used for some segments and the helicopter mode is used for others, the same segmentation as outlined above applies because helicopter operations must still conform to the AEDT procedural step rules. To facilitate hybrid modeling, point-to-point operations using only the fixed-wing mode follow the same segmentation as that used for helicopter departure, overflight, and approach operations. In doing so, the prior fixed-wing approach of using departure-only operations is abandoned. Note, however, that it is possible to arbitrarily segment point-to-point operations in the fixed-wing mode because the helicopter procedural step rules do not apply.

1. Operational Mode Violations

In the analysis of Gen 1 and Gen 2 route data, two operations were identified for which no existing helicopter procedural steps exist. These are a decelerating climb and an accelerating descent. The operations occur on an infrequent basis, but nevertheless must be addressed.

The case of a decelerating climb is illustrated in the Gen 1 route from KDF4 to KDT4 in Figure 12. This occurs at the start of the overflight segment. The lack of an existing operational mode is overcome with a combination of a mode D segment to increase altitude while maintaining speed, followed by a short level segment (L) maintaining both altitude and speed, followed by a mode B segment to maintain altitude while decelerating. According to Figure 9, it is also possible to use just two segments (D followed by B), but that approach is not adopted here.

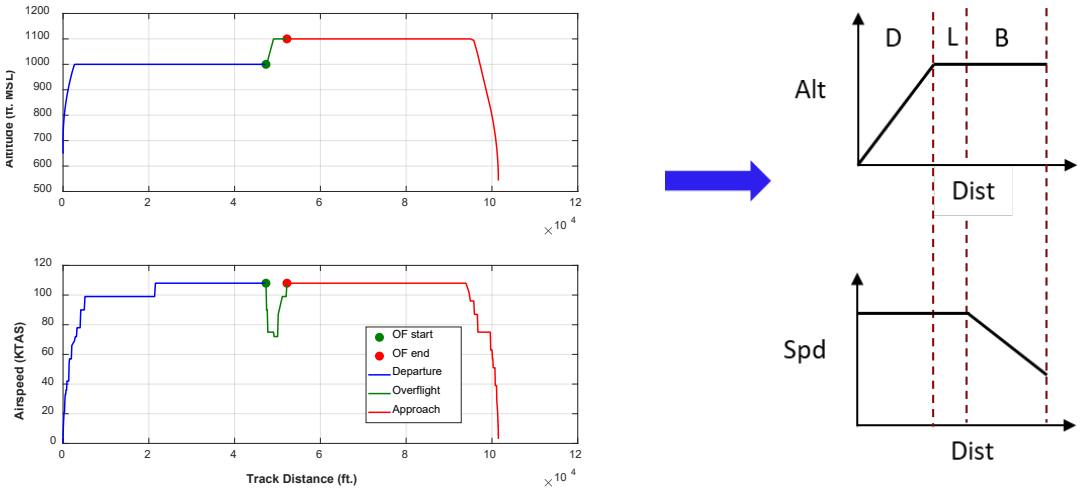

Figure 12: Illustration of decelerating climb at start of overflight segment (left). Use of existing modes D, L, B achieves the desired operation between start and finish (right).

The case of an accelerating descent is illustrated in the Gen 2 route from DF29 to DF1 in Figure 13. This occurs in the overflight segment at a track distance of about 65k ft. The deficiency is overcome with a combination of a mode A segment to reduce altitude while maintaining speed, followed by a short level segment (L) maintaining both altitude and speed, followed by a mode E segment to maintain altitude while accelerating. As for the decelerating climb case, it is also possible to use just two segments (A followed by E), but that approach is not adopted here.

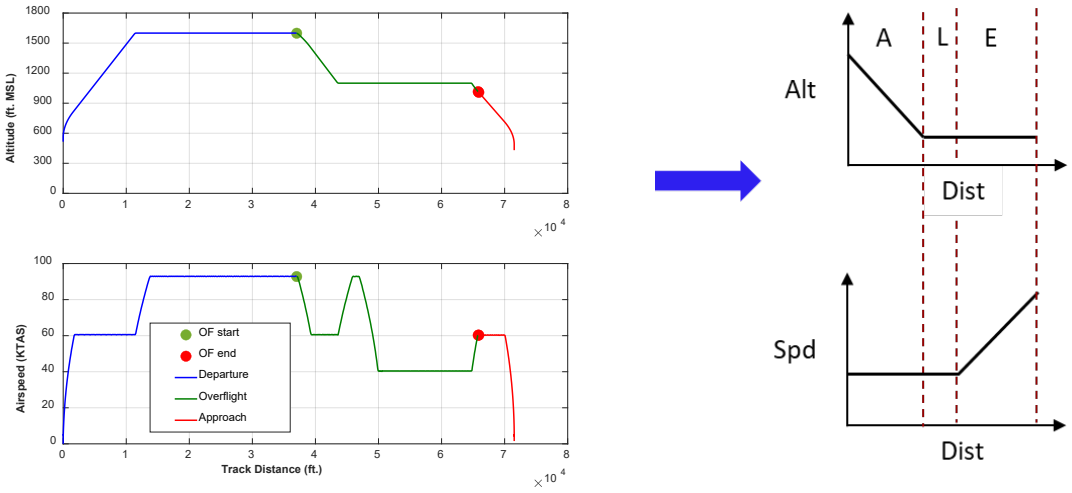

Figure 13: Illustration of accelerating descent at about 65k ft. (left).
Use of existing modes A, L, E achieves the desired operation between start and finish (right).

C. Casting

Following segmentation, flight profiles for each operation (departure, overflight, and approach) are cast segment-by-segment into a set of procedural steps that adhere to AEDT rules. Because the Gen 1 and Gen 2 route data do not include ground or flight idle conditions and these procedural steps are required at the beginning of departure operations and the end of approach operations, very short duration (1 s) steps are added to adhere to the rules and not significantly contribute to the noise exposure.

In the process of casting, any procedural modes in Table 1 may be specified except for *taxi at constant speed* (T). Segments that are cast to procedural steps that lack NPD data, namely, modes B, C, E, F, G, I, V/W, and Y/Z in the present work, are nevertheless cast to those steps. Internal to AEDT, missing NPD data are substituted according to Table 1. Note that neither the Gen 1 or 2 routes include hover modes I or J.

D. AEDT Study Construction

In the construction of the AEDT study, each operation (departure, overflight, and approach) has a set of tracks that is largely unaltered from the fixed-wing tracks except for segmentation. Each helicopter operation has an accompanying flight profile consisting of the cast set of procedural steps, and each fixed-wing operation has an accompanying fixed-point profile obtained from the segmented fixed-point profile used for the point-to-point departure operation. The AEDT operational group combines the three operations (departure, overflight, and approach) into a single point-to-point flight. The AEDT uses annualizations to specify a set of operational groups to be included in noise metrics calculations.

IV. Results

Thirteen point-to-point operations from the Gen 1 route structure[4] in the Dallas-Ft. Worth, TX, area were modeled in AEDT in four different ways; one using fixed-wing mode for departure, overflight, and approach segments (FFF), one using helicopter mode for departure, overflight, and approach segments (HHH), and two using two hybrid approaches, FHF and HFH. Other hybrid mode variations, e.g., FFH, are possible but are not considered herein. It should be noted that the choice of modeling point-to-point operations as FFF or HHH may be driven by number of considerations, including availability of requisite NPD data. On the other hand, hybrid modeling may be best reserved for investigative purposes because of its added complexity and the need for both fixed-wing and helicopter NPD data. The route structure is shown in Figure 14. Each location has both a runway and a helipad to

support both fixed-wing and helicopter operations. Local terrain was included in the analyses and the total study area was 1,225 square nautical miles (nm).

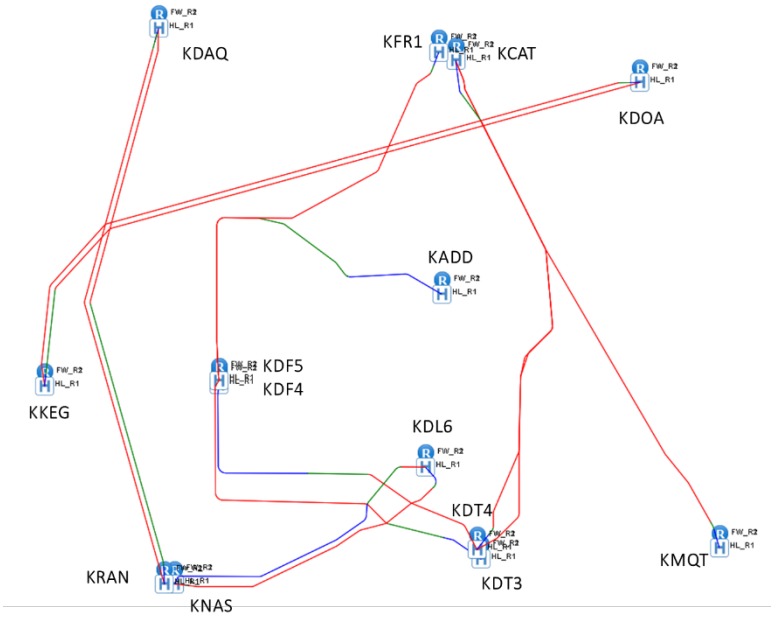

Figure 14: Thirteen point-to-point operations from the Gen 1 route structure.[4] Each operation is comprised of a departure segment (in blue), an overflight segment (in green), and an approach segment (in red).

A. Single Event Analyses

The four modeling variants were exercised on the route from KADD to KDF5. This route was selected because the lengths of the departure, overflight, and approach segments were well-balanced. Sound exposure level contours for the FFF modeling variant are shown in Figure 15. Departure, overflight, and approach segments are depicted as dashed blue, green, and red lines, respectively. As in prior work,[4,5] the highest levels are found in the landing area. Levels are generally several decibels lower than prior work due to updates made in the Gen 3.1.2 NPD data.[6] The dipole directivity used in the AEDT noise fraction adjustment is most apparent in the landing area, and nonuniformities on either side of the track are due solely to the summation of noise contributions from neighboring segments. This is most noticeable on the inside corner of the turn to the south toward KDF5. In contrast, segments modeled in helicopter mode have narrower contours than those modeled in fixed-wing mode. For example, compare contours shown in Figure 16 with those shown in Figure 15. Overall, differences between FFF and HHH modeling are due to the combined effects of how the operations were cast, the AEDT lateral directivity adjustment for helicopters (recall the discussion related to Figure 5), and the necessity of having to select just 3 NPD curves (not including flight idle and hover) associated with a limited number of available helicopter procedural steps, from the 42 NPD curves used for fixed-wing analyses. As shown in Figure 6, a different selection of operating states for helicopter modes A and D (and to a lesser extent mode L, not shown) could significantly change the result. It should be noted that because the vehicle is modeled as a propeller-driven aircraft in fixed-wing mode, the airplane shielding and engine installation effect component of the AEDT lateral attenuation adjustment is zero, making the total lateral attenuation adjustment the same for helicopter and fixed-wing modes. In other words, the lateral attenuation adjustment does not contribute to the differences shown.

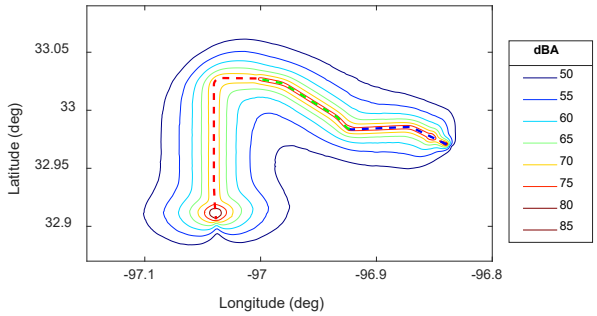

Figure 15: Sound exposure level (L_{AE}) for FFF modeling variant on route KADD-KDF5.

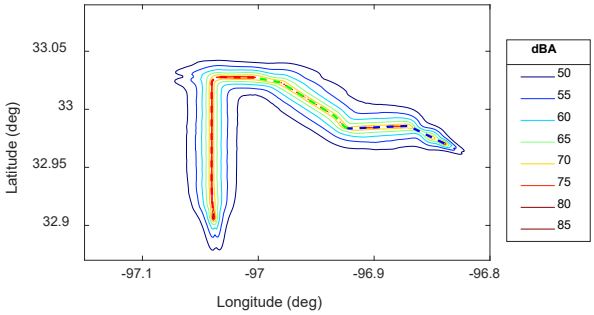

Figure 16: Sound exposure level (L_{AE}) for HHH modeling variant on route KADD-KDF5.

Sound exposure level contours for the hybrid modeling approaches, FHF and HFH, shown in Figure 17 and Figure 18, respectively, clearly resemble the characteristics of the departure, overflight, and approach segments. The transitions between operational segments appear smooth.

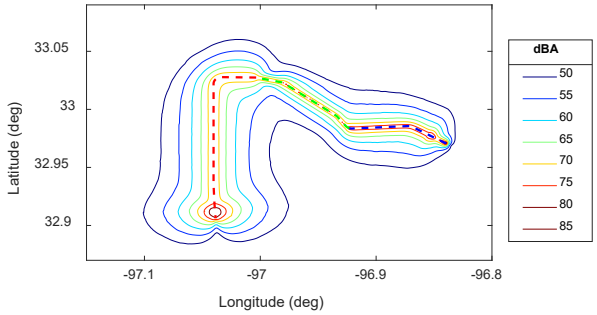

Figure 17: Sound exposure level (L_{AE}) for FHF modeling variant on route KADD-KDF5.

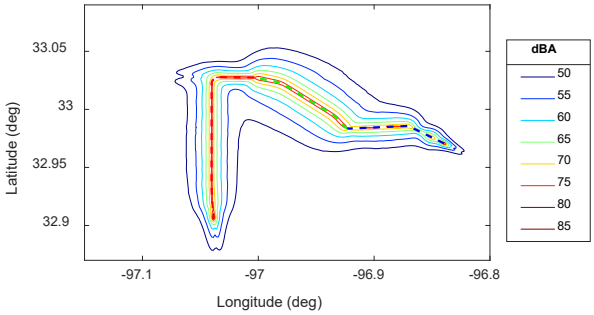

Figure 18: Sound exposure level (L_{AE}) for HFH modeling variant on route KADD-KDF5.

How differences between modeling approaches vary along the route are more clearly seen by subtracting sound exposure levels. The HHH modeling variant differs the most overall relative to the FFF variant, see Figure 19. Again, recalling the discission related to Figure 5, levels beneath the flight track in the cruise portion compare most favorably, then vary with distance astride the track. Differences are greatest in the takeoff and landing areas, where the majority of fixed-wing NPDs are encountered but where only 1 NPD for each departure (D) and approach (A) procedural step is allowed in helicopter mode. Levels in the takeoff area differ by as much as ±10 dBA, and those in the landing area are as much as 15 dBA lower for the HHH variant relative to the FFF variant. Differences between the FHF and FFF modeling variants, shown in Figure 20, are mostly limited to the overflight segment, with nearly a 10 dBA difference near the transition from overflight to approach. As expected, differences between the HFH and FFF modeling variants, shown in Figure 21, lie between those in Figures 19 and 20.

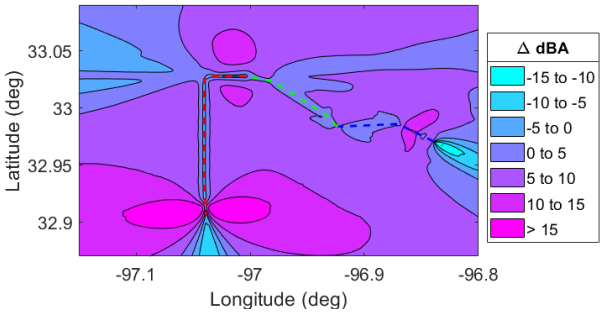

Figure 19: Difference in L_{AE} (FFF-HHH) on route KADD-KDF5.

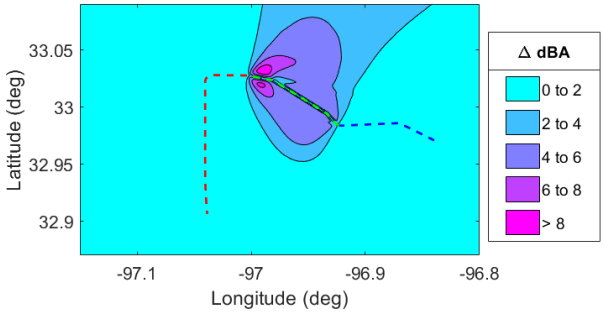

Figure 20: Difference in L_{AE} (FFF-FHF) on route KADD-KDF5.

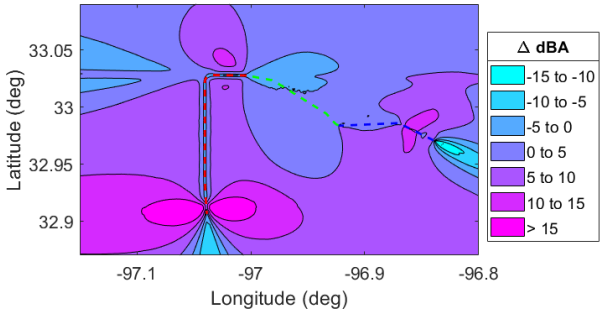

Figure 21: Difference in L_{AE} (FFF-HFH) on route KADD-KDF5.

B. Fleet Analyses

Day-night average sound level (L_{dn}) exposure maps were generated for the routes shown in Figure 14. Each route had 600 daily operations, all during the daytime period between 7AM and 10PM. Results for each of the modeling variants are shown in Figures 22 – 25. As was the case for the single event analyses, fleet analyses modeled with a greater portion of fixed-wing operational segments show higher cumulative exposure than those with a greater portion of helicopter operational segments. Further, the exposures in the takeoff and landing areas are greatly reduced for the HFH and HHH cases.

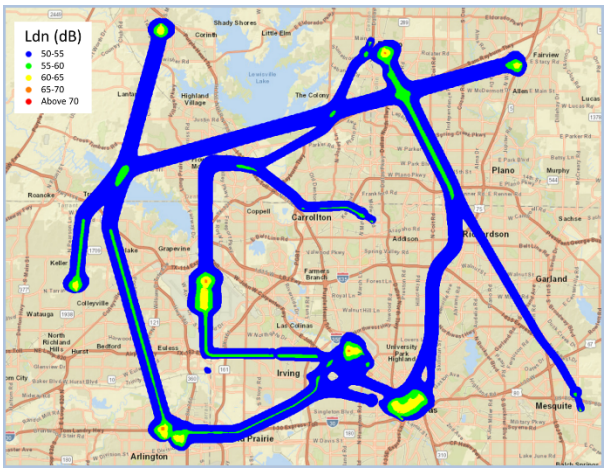

Figure 22: Map of L_{dn} for FFF modeling variant.

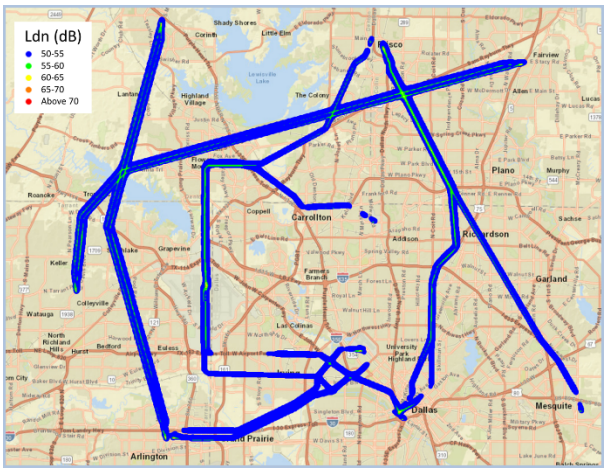

Figure 23: Map of L_{dn} for HHH modeling variant.

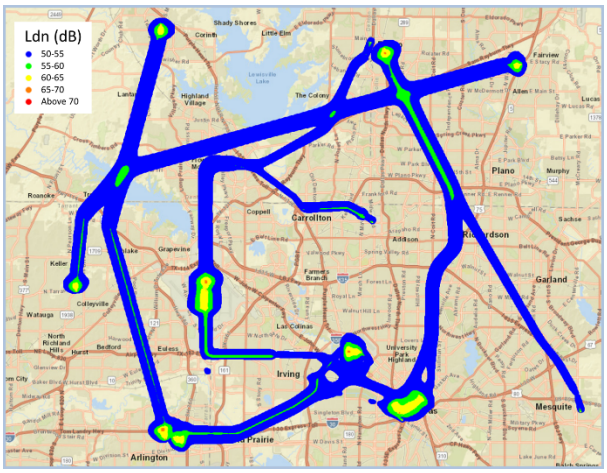

Figure 24: Map of L_{dn} for FHF modeling variant.

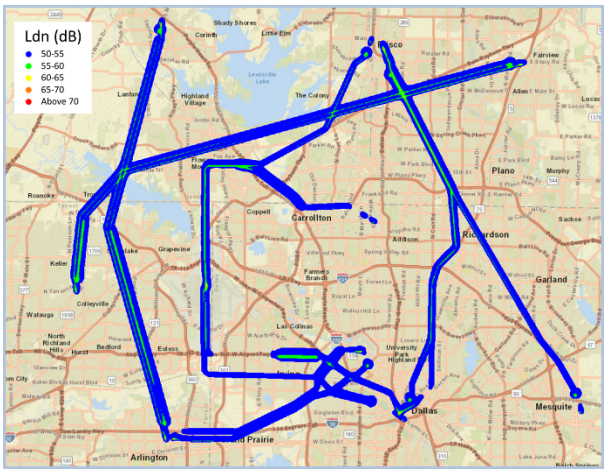

Figure 25: Map of L_{dn} for HFH modeling variant.

Contour areas provide a compact means of comparing fleet analysis results among modeling variants, see Table 3. Consistent with the visual observation, the FHF variant captures a majority of the FFF variant contour area, with decreasing areas for the HFH and HHH variants. The large differences between FFF and HFH, and between FFF and HHH, at the highest exposure levels, i.e., those near takeoff and landing areas, indicate that the particular selection of helicopter modes D and A NPD data used in this work underestimated the exposure for these particular operations relative to the fixed-wing analyses. As an aside, note that the FFF exposure areas for levels above 55 L_{dn} are somewhat lower than those previously computed in the Gen 1 fleet analyses[4] (not shown) because of the lower noise levels in the Gen 3.1.2 NPD data used in the present work, and because only 13 of 16 routes were included in the present work.

Table 3: Comparison of L_{dn} exposure areas for different modeling variants.

L_{dn} Exposure Level (dB)	FFF Exposure Area (sq nm)	Percentage of FFF Exposure Area		
		FHF	HFH	HHH
50-55	110	93	49	43
55-60	19.4	84	48	34
60-65	3.90	98	4	4
65-70	0.13	100	13	13

V. Concluding Remarks

A method was presented for evaluating UAM vehicle community noise using the FAA Aviation Environmental Design Tool in helicopter mode. To overcome limitations in the number and usage of operational mode procedural steps, point-to-point routes were segmented into departure, overflight, and approach operations and workarounds were offered for helicopter operations lacking defined AEDT procedural steps, e.g., decelerating climb. The helicopter approach has an advantage over the prior fixed-wing approach using fixed-point flight profiles as it requires a lesser amount of noise-power-distance data, albeit with compromises for modeling noise that changes significantly over the course of an operation. A hybrid modeling approach that allows some operational segments to be modeled in fixed-wing mode and others in helicopter mode was shown to be compatible with the AEDT and yield exposure results that fell between two single aircraft mode variants. With this capability in hand, AEDT modeling results using fixed-wing and helicopter approaches may be compared with simulation data to identify best practices for modeling UAM operations within AEDT.

Acknowledgments

This work was supported by the NASA Aeronautics Research Mission Directorate, Revolutionary Vertical Lift Technology Project. The authors wish to thank Eric Boeker and Bradley Nicholas of the U.S. Department of Transportation Volpe National Transportation Systems Center for their consultation during the development of the AEDT modeling methodology discussed in this paper.

References

[1]"Aviation Environmental Design Tool (AEDT) technical manual, Version 3e," U.S. Department of Transportation, Volpe National Transportation Systems Center DOT-VNTSC-FAA-22-04, Cambridge, MA, 2022.

[2]Maurice, L.Q., Lee, D.S., Wuebbles, D.W., Isaksen, I., Finegold, L., Vallet, M., Pilling, M., and Spengler, J., *Final report of the International Civil Aviation Organization (ICAO) Committee on Aviation and Environmental Protection (CAEP) Workshop*, Assessing current scientific knowledge, uncertainties and gaps in quantifying climate change, noise and air quality aviation impacts, L.Q. Maurice, et al., Editors. 2009, US Federal Aviation Administration and Manchester Metropolitan University, : Washington, DC and Manchester, UK.

[3]Rizzi, S.A., et al., "Urban air mobility noise: Current practice, gaps, and recommendations," NASA TP-2020-5007433, 2020.

[4]Rizzi, S.A. and Rafaelof, M., "Community noise assessment of urban air mobility vehicle operations using the FAA Aviation Environmental Design Tool," *InterNoise 2021*, Virtual Meeting, 2021.

[5]Rizzi, S.A. and Rafaelof, M., "Second generation UAM community noise assessment using the FAA Aviation Environmental Design Tool," *AIAA SciTech Forum*, AIAA-2022-2167, San Diego, CA, 2022, https://arc.aiaa.org/doi/10.2514/6.2022-2167.

[6]Rizzi, S.A., Letica, S.J., Boyd Jr., D.D., and Lopes, L.V., "Prediction-based approaches for generation of noise-power-distance data with application to urban air mobility vehicles," *Submitted to the AIAA Journal of Aircraft*, 2023.

[7]Lopes, L.V. and Burley, C.L., "ANOPP2 user's manual: Version 1.2," NASA TM-2016-219342, 2016.

[8]Patterson, M.D., Antcliff, K.R., and Kohlman, L.W., "A proposed approach to studying urban air mobility missions including an initial exploration of mission requirements," *AHS International 74th Annual Forum and Technology Display*, Phoenix, AZ, 2018.

[9]Silva, C., Johnson, W.R., Solis, E., Patterson, M.D., and Antcliff, K.R., "VTOL urban air mobility concept vehicles for technology development," *AIAA AVIATION Forum*, AIAA-2018-3847, Atlanta, GA, 2018, https://doi.org/10.2514/6.2018-3847.

[10]Johnson, W.R., "Rotorcraft aerodynamic models for a comprehensive analysis," *AHS International 54th Annual Forum*, Washington, DC, 1998.

[11]Farassat, F. and Succi, G., "The prediction of helicopter rotor discrete frequency noise," *Vertica*, Vol. 7, 1983, pp. 309-320.

[12]Lopes, L.V., "ANOPP2's Farassat formulations internal functional modules (AFFIFMs) reference manual, Version 1.4," NASA TM-20210021111, 2021.

[13]Lopes, L.V., "Compact assumption applied to monopole term of Farassat's formulations," *AIAA Journal of Aircraft*, Vol. 54, No. 5, 2017, pp. 1649-1663, https://doi.org/10.2514/1.C034048.

[14]Brooks, T.F., Pope, D.S., and Marcolini, M.A., "Airfoil self-noise and prediction," NASA RP-1218, 1989.

[15]"Aviation Environmental Design Tool (AEDT) user manual, Version 3e," U.S. Department of Transportation, Volpe National Transportation Systems Center DOT-VNTSC-FAA-22-03, Cambridge, MA, 2022.

[16]"Noise modeling methods for urban air mobility vehicles in the Federal Aviation Administration's Aviation Environmental Design Tool," U.S. Department of Transportation, Volpe National Transportation Systems Center DOT-VNTSC-NASA-22-02, Cambridge, MA, 2022.